energies

MDPI

Article

A Coordinated Voltage Regulation Algorithm of a Power Distribution Grid with Multiple Photovoltaic Distributed Generators Based on Active Power Curtailment and On-Line Tap Changer

Yassir Maataoui [1], Hamid Chekenbah [1], Omar Boutfarjoute [1], Vicenç Puig [2,*] and Rafik Lasri [1]

[1] TED:AEEP, FPL, Abdelmalek Essaadi University, Tetouan 93000, Morocco; maataoui.yassir@gmail.com (Y.M.); hamid.chekenbah@gmail.com (H.C.); omarboutfarjoute@gmail.com (O.B.); r.lasri@uae.ac.ma (R.L.)
[2] Supervision, Safety and Automatic Control Research Center (CS2AC), The Universitat Politécnica de Catalunya, Rambla Sant Nebridi, 22, 08222 Barcelona, Spain
* Correspondence: vicenc.puig@upc.edu

Abstract: The aim of this research is to manage the voltage of an active distribution grid with a low X/R ratio and multiple Photovoltaic Distributed Generators (PVDGs) operating under varying conditions. This is achieved by providing a methodology for coordinating three voltage-based controllers implementing an Adaptive Neuro-Fuzzy Inference System (ANFIS). The first controller is for the On-Line Tap Changer (OLTC), which computes its adequate voltage reference. Whereas the second determines the required Active Power Curtailment (APC) setpoint for PVDG units with the aim of regulating the voltage magnitude and preventing continuous tap operation (the hunting problem) of OLTC. Finally, the last component is an auxiliary controller designed for reactive power adjustment. Its function is to manage voltage at the Common Coupling Point (CCP) within the network. This regulation not only aids in preventing undue stress on the OLTC but also contributes to a modest reduction in active power generated by PVDGs. The algorithm coordinating between these three controllers is simulated in MATLAB/SIMULINK and tested on a modified IEEE 33-bus power distribution grid (PDG). The results revealed the efficacy of the adopted algorithm in regulating voltage magnitudes in all buses compared to the traditional control method.

Keywords: power distribution grid; Photovoltaic Distributed Generator; neuro-fuzzy; On-Line Tap Changer (OLTC); tap hunting; active power curtailment; voltage control; voltage regulation

Citation: Maataoui, Y.; Chekenbah, H.; Boutfarjoute, O.; Puig, V.; Lasri, R. A Coordinated Voltage Regulation Algorithm of a Power Distribution Grid with Multiple Photovoltaic Distributed Generators Based on Active Power Curtailment and On-Line Tap Changer. *Energies* **2023**, *16*, 5279. https://doi.org/10.3390/en16145279

Academic Editor: Salman Mohagheghi

Received: 13 June 2023
Revised: 4 July 2023
Accepted: 7 July 2023
Published: 10 July 2023

1. Introduction

The stability and safety of Power Distribution Grids (PDGs) rely heavily on voltage regulation. The purpose of this regulation is to maintain the voltage within a standard range of $0.95 \leq V$ to ≤ 1.05 V set by distribution grid operators (DGOs) [1]. One of the essential parts of operating and controlling distribution grids is maintaining voltage stability. Low voltage magnitudes can potentially cause more current draw and lead to equipment damage [2], whereas high voltage magnitudes result in increased transformer losses and high power dissipation in induction devices [3]. In distribution grids, the step up or step down of the voltage is carried by an On-Line Tap Changer (OLTC), which is embedded into the main tank of the transformer located at the substation [4]. OLTC maintains the voltage magnitudes of the passive grids within standard limits by controlling the voltage of the bus located at the substation to be the highest and approximately equal to a fixed voltage reference [5]. The traditional voltage regulation method used by the OLTC is poorly affected by the integration of intermittent Photovoltaic Distributed Generators (PVDGs) into the distribution grid [6]. Since there is a high amount of current flowing in the opposite direction, the highest voltage magnitude in the grid is no longer at the substation bus [7]. As the traditional OLTC voltage regulation assumes the substation voltage to be

the greatest, connecting multiple intermittent PVDGs will cause overvoltage at the grid buses [8].

The integration of Renewable Energy Sources (RESs) into power distribution grids has experienced exponential growth in recent years. Particularly with the advent of photovoltaic (PV) and wind energy technologies, the implementation of RESs in Power Distribution Grids (PDGs) can lead to numerous benefits. These advantages include a decrease in line losses within the network, meeting increased load demands, and deferring substantial investments necessary for the expansion of transmission and distribution network capacities.

Despite the significant benefits, challenges arise when intermittent Photovoltaic Distributed Generators (PVDGs) are introduced into PDGs. One major challenge is the difficulty of maintaining voltage regulation, especially in scenarios where high voltage is generated by reversed power flow. This phenomenon is observed when the power generated by intermittent PVDGs exceeds the power consumption of the load on the feeder [9,10]. Such a situation can create complexities in the efficient management of the PDG.

In distribution grids that have a low X/R ratio, the voltage-to-active power sensitivity is significantly higher than the voltage-to-reactive power sensitivity [11]. As a result, active power generated by intermittent PVDGs is much more effective than reactive power in reducing overvoltage [12], and reactive power compensation by DGs is constrained by the power factor. Since a multitude of devices are connected to the active distribution grid, it is crucial to implement an effective voltage regulation system for it, as the traditional OLTC control method is ineffective in limiting high voltage magnitudes and fluctuations caused by intermittent PVDGs.

In the published literature, several methods have been proposed to mitigate voltage violations. In [12–16], many coordinated voltage regulation strategies have been developed for distribution networks, including PVDGs and Energy Storage System (ESS) technologies. A new management methodology for OLTC and Photovoltaic (PV) smart inverters is proposed in [17] to improve the quality of distribution systems with a high penetration of solar PV systems. The proposed scheme computes the adequate OLTC tap position based on the active power of PVs. Ref. [18] has also suggested using DG units, capacitor banks (CBs), and a transformer with tap-changing capabilities to enhance the voltage quality. The OLTC, CBs, PVs, and Battery ESS plants can all work together efficiently, according to [19], which suggests a coordinated active and reactive power optimization strategy for distribution networks.

The deloading strategy for PV power plants is employed as a measure to ensure grid stability and reliability, akin to the deloading procedure utilized for frequency control [20]. This approach deliberately diminishes the power output of PV power plants. The principal objective, however, is to maintain voltage levels within permissible boundaries, as opposed to controlling the grid frequency.

In a study by [21], the authors addressed the issue of overvoltage in power networks resulting from the integration of PV units. They recommended implementing demand response (DR) programs and load-shifting techniques to regulate voltage levels during periods of high demand. Another study [22] proposed a distributed control plan for Battery Energy Storage Systems (BESS) to tackle voltage regulation in the distribution grid during peak PV generation. The proposed strategy amalgamates a local droop-based control method and a distributed control scheme to manage battery storage charging and discharging, ensuring voltage along the feeder remains within acceptable limits.

The most straightforward approaches to maintaining voltage within a specified range involve curtailing Distributed Renewable Energy Source (DRES) production to mitigate overvoltage issues. For instance, the reduction of active power in photovoltaic inverters, as depicted in [23], is used to address overvoltage situations.

In addition, there have been multiple intelligent methods in the literature that try to control the voltage profile when intermittent PVDGs are connected to power distribution grids. Adaptive Neuro-Fuzzy Inference Systems (ANFIS), Artificial Neural Networks

(ANN), and Fuzzy Inference Systems (FIS) are just some examples of the intelligent methods currently in use. These intelligent systems are robust to the uncertainty of system dynamics and can function without an accurate model of the power grid [24]. In [25,26], voltage regulation of a power distribution system is accomplished via fuzzy logic control (FLC). While [27] uses FLC and gain scheduling for microgrid-scale distributed voltage control. In [28], three fuzzy logic controllers—one for OLTC tap operation, a second one for DGs reactive power, and a last one for Active Power Curtailment (APC)—are proposed to address the voltage magnitude violation. The control of voltage in distribution systems using an artificial neural network (ANN) is presented in [29]. However, the creation of the FLC system needs an appropriate rule base for decision-making, fitting scaling factors, and adjusting membership functions. In addition, to achieve high-quality results from ANN-based controllers, proper data training is needed.

In order to manage the voltage at the CCP during grid faults, two ANFIS controllers are proposed in [30], the first to control the PV inverter's injection and absorption of reactive power and the second to regulate the charge and discharge of the ESS. However, only one PV system and one ESS are considered in this study.

This paper proposes an ANFIS-based voltage control method for coordinating OLTC operation and the power output of intermittent PVDGs. Thus, the main contributions of this paper are as follows:

1. A novel OLTC voltage regulation controller based on ANFIS (ANFIS-OC) that considers the minimum and maximum voltages across the power distribution grid to compute the adequate reference voltage;
2. A novel APC controller based on ANFIS (ANFIS-APCC) determines the optimal active power curtailment setpoint of PVDG units.
3. To regulate voltage at the Common Coupling Point (CCP) with the distribution network and minimize the frequent tap operation of the On-Load Tap Changer (OLTC), an auxiliary controller for reactive power adjustment, the Adaptive Neuro-Fuzzy Inference System for Reactive Power Adjustment Controller of Inverters (ANFIS-RPAC), is proposed. This system also aims to minimize the reduction in active power generated by Photovoltaic Distributed Generators (PVDGs).
4. A coordination approach is proposed between ANFIS-OC, ANFIS-APCC, and the auxiliary ANFIS-RPCC controllers to prevent continuous tap hunting of the OLTC and to minimize the active power reduction on PVDGs.

The subsequent structure of this article is as follows: Section 2 examines the impact of the operation of OLTCs and PVDGs on voltage regulation. Section 3 is dedicated to the design of the proposed control algorithms. Section 4 discusses the results obtained. Finally, the main conclusions are presented in the last section.

2. On-Line Tap Changer Operation and Intermittent Photovoltaic Distributed Generator Units in Voltage Regulation

2.1. On-Line Tap Changer

The OLTC is the most efficient equipment used for changing voltage magnitudes in power distribution grids. It can maintain a constant output voltage of the substation transformer as the input voltage and load variations change. Its effectiveness comes from its capacity to control the voltage magnitude of several feeders [31,32]. In order to maintain the transformer's output voltage equal to the fixed voltage magnitude while the input voltage and the network load vary, the OLTC modifies the transformer winding ratio. The OLTC operation without the compounding function is illustrated in Figure 1.

$$V_{MV} = \frac{1}{r} V_{HV} - \frac{r Z_T(r) S}{V_{HV}^*} \tag{1}$$

$$r = \frac{V_{HV}}{V_{MV}} \tag{2}$$

where V_{HV}, V_{MV}, and r are the high bus voltage magnitude, medium bus voltage, and transformer turn's ratio, respectively. $Z_T(r)$ is the transformer impedance, and S is the apparent power transmitted to the load [33].

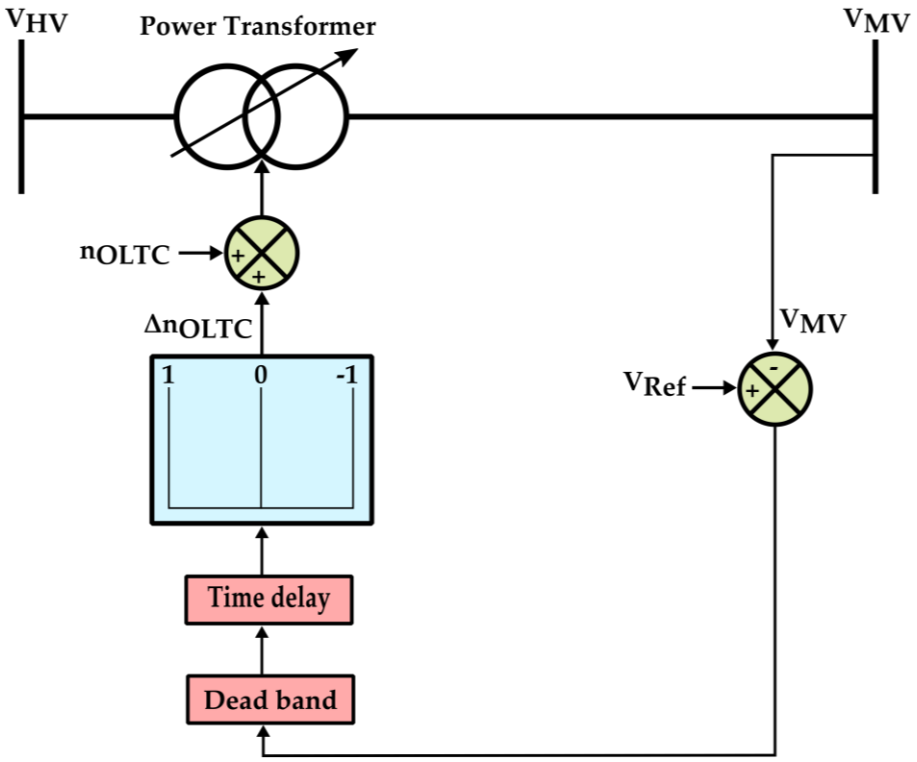

Figure 1. OLTC operation.

From Equations (1) and (2), the medium bus voltage magnitude V_{MV} is dependent on the transformer turn's ratio r, which is automatically adjusted by a discrete step corresponding to a change of tap Δn_{OLTC}. Therefore, the V_{MV} voltage magnitude can be regulated.

Continuously monitoring the voltage at the substation bus and maintaining it at a constant voltage magnitude makes the OLTC unable to successfully deal with increasing and varying voltages introduced by intermittent DGs when they are connected to the power grid [34].

2.2. Photovoltaic Distributed Generators

Distribution grids face several difficulties when PVDGs generate high active power. These difficulties include rising voltages above acceptable bounds, continuous voltage magnitude changes, and bi-directional power flow [35,36].

Equations (3)–(6) show the impact of intermittent PVDGs on voltage magnitudes between a substation bus and a PVDG's bus, where ΔV is the voltage drop, V_{MV} is the voltage magnitude at the bus located after the power transformer, Vpv_{DG} is the voltage magnitude where DG is connected to the grid, and R and X are the resistance and the reactance of the line, respectively. P_L and Q_L are the active and reactive power of the load, respectively; Qpv_{DG} is the reactive power supplied by DG, and Ppv_{DG} is the generated active power by PVDG [37]. Figure 2 illustrates a distribution grid with a reversal of power flow.

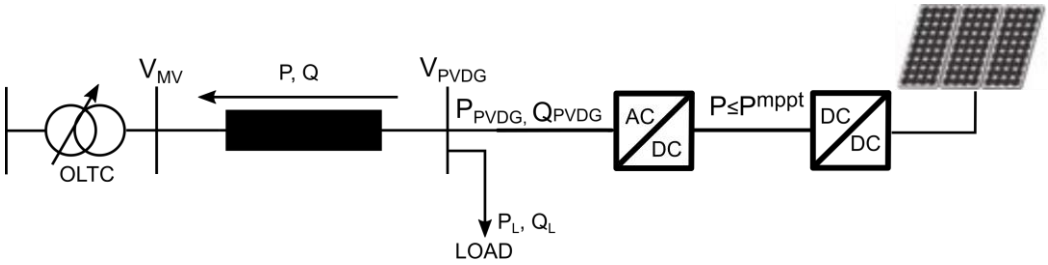

Figure 2. Basic configuration of a distribution grid involving PVDG.

A passive distribution grid without a PVDG connection is represented in Equation (3), which can be further reduced to Equation (4) since the quadrature term of ΔV is negligible.

$$\Delta V = \Delta V_d + j\Delta V_q = \frac{R \cdot P_L + X \cdot Q_L}{V_{MV}} + j\frac{X \cdot P_L - R \cdot Q_L}{V_{MV}} \tag{3}$$

$$\Delta V \approx \ \Delta V_d \approx \frac{R \cdot P_L + X \cdot Q_L}{V_{MV}} \tag{4}$$

Equation (5) represents a distribution grid with a connected PVDG. Since the voltage variation ΔV depends on the output power of PVDG, the voltage will change regularly as the P_{PVDG} and Q_{PVDG} generation change in response to different weather conditions.

$$\Delta V \approx \Delta V_d \approx \frac{R \cdot (P_{PVDG} - P_L) + X \cdot (Q_{PVDG} - Q_L)}{V_{PVDG}} \tag{5}$$

As the linear resistance is more significant than the linear reactance $R >> X$ in the distribution grid, the reactive power generated by intermittent PVDGs is negligible in voltage regulation.

$$\Delta V \approx \frac{R \cdot (P_{PVDG} - P_L)}{V_{PVDG}} \tag{6}$$

3. Adaptive Neuro-Fuzzy Inference System Controller

In this study, a Takagi-Sugeno adaptive neuro-fuzzy inference system (ANFIS) is designed to control the voltage in a power distribution grid. It is based on the parallel data processing capabilities of artificial neural networks and the capabilities of fuzzy inference systems to select the rules and parameters of membership functions (MFs). The general architecture of a 5-layer ANFIS is illustrated in Figure 3.

It has two inputs (m and n) and an output (q), which is a linear combination of these, and three membership functions for each input, making the number of rules equal to nine. Furthermore, the different layers in the ANFIS architecture are described as follows:

Layer 1: The adaptive fuzzification layer consists of membership functions and input variables. Each node in the first layer is an adaptive node that performs a function.

$$O_{1,i} = \mu_{Ai}(n) \ and \ O_{1,i} = \mu_{Bi}(m) \ where \ i = 1, 2, 3 \tag{7}$$

where A_i and B_i are the linguistic labels associated with node i for each input, $O_{1,i}$ and $O_{2,i}$ are the membership functions. In this study, $\mu_{Ai}(n)$ and $\mu_{Bi}(m)$ are defined as the triangular membership functions given by (8):

$$\mu_{Ai}(n), \mu_{Bi}(m) = \begin{cases} 0, & if \ n, m \leq \alpha \ ; n, m \geq \gamma \\ \dfrac{n, m - \alpha}{\beta - \alpha}, & if \ \alpha \leq n, m \leq \beta \\ \dfrac{\gamma - n, m}{\gamma - \beta}, & if \ \beta \leq n, m \leq \gamma \end{cases} \tag{8}$$

Based on this equation, the triangular membership function depends on three parameters: α, β, and γ. Figure 4 shows a triangular membership function in which the learning process adaptively tunes its parameters.

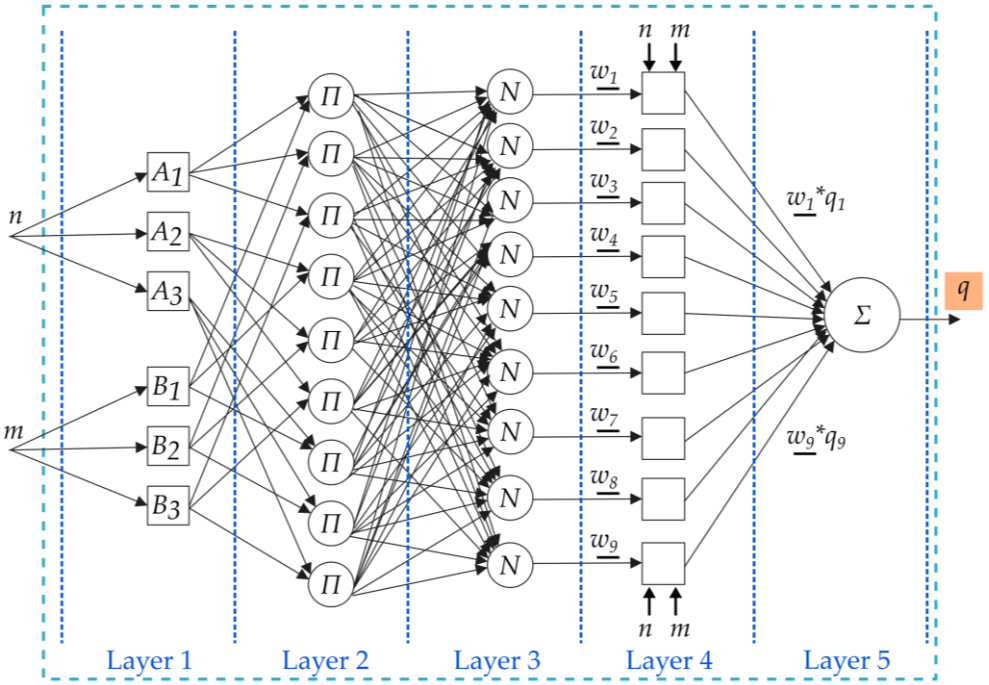

Figure 3. ANFIS architecture.

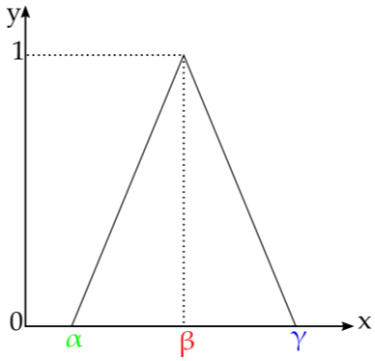

Figure 4. Triangular membership function.

Layer 2: Each fixed node multiplies the incoming signals to approximate the forwarded output that represents the corresponding rules.

Layer 3: For each normalized node, the firing strength layer calculates a weight.

$$\underline{W_i} = \frac{W_i}{W_1 + W_2 + \cdots + W_9} \qquad where\ i = 1, 2, \ldots, 9 \tag{9}$$

Layer 4: Normalized outputs from each neuron are generated by the adaptive implication layer, which operates by following inference rules.

$$O_{4,i} = \underline{W_i}\ q_i = W_i\, r_i \qquad where\ i = 1, 2, \ldots, 9 \tag{10}$$

Layer 5: To produce a clear result, the output layer combines all of the signals provided by the previous layers.

$$O_{5,i} = \sum_{i=1}^{9} \underline{W_i} * q_i \tag{11}$$

3.1. ANFIS-Based OLTC Controller

Multiple difficulties, such as higher voltage magnitudes, voltage variations, and reversal power flow, arise due to the high integration of DGs that use renewable energy sources. The traditional approach of OLTC voltage regulation, which is based on a preset voltage magnitude with its most significant point at the substation bus, was developed for power distribution grids with unidirectional power flow. This approach to voltage regulation becomes ineffective when the power flows both ways and the output power of the DGs fluctuates. Thus, the main OLTC may not regulate the overall voltage magnitude in the network.

Therefore, this study develops an intelligent ANFIS-based OLTC control algorithm that will regulate the voltage magnitude when DGs are connected across the power distribution grid. It will compute the optimal reference voltage magnitude in such a manner that the extreme voltages at critical sites like the substation bus, end of feeder, and DGs buses are kept within the standard voltage range of $0.95 \leq V \leq 1.05$. This minimizes voltage deviations at all buses in the power distribution grid. Figure 5 shows the proposed ANFIS-based OLTC controller. V_{max} and V_{min} are two inputs provided for the controller measured only from critical sites (the buses of the substation, DGs terminals, and the ends of feeders) in order to minimize the number of measuring devices and their required communication infrastructure. Based on these two inputs, the controller-based ANFIS will compute the optimal reference voltage magnitude and send the control signal to OLTC, which will adjust its tap settings to regulate the voltage at all grid feeders.

Figure 5. Structure of ANFIS-OC.

3.2. ANFIS-Based PVDG Reactive Power Adjustment Controller

An auxiliary controller is designed for reactive power adjustment. Its function is to regulate locally the voltage at CCP within the network. This regulation not only aids in preventing undue stress on the OLTC but also contributes to a modest reduction in active power generated by PVDGs. Figure 6 shows the proposed ANFIS-based reactive power adjustment controller.

The controller has as input the voltage magnitude $V_{DG}(i)$ at CCP with the PDG. The output $\Delta Q_{PVDG}(i)$ is the reactive power setpoint provided for a specified PV inverter. The maximum reactive power adjustment $\Delta Q^{max}_{PVDG(i)}$ produced by the ith PVDG is constrained by the PV inverter power factor as well as its reactive power capability curves. This can be evaluated through:

$$\Delta Q^{IN}_{PVDG(i)} = \sqrt{S^2_{IN} - \left(P_{PVDG(i)} - \Delta P_{PVDG(i)}\right)^2} \tag{12}$$

$$\Delta Q^{PF}_{PVDG(i)} = P_{PVDG(i)} \tan\left(cos^{-1}\left(pf_{PVDG(i)}\right)\right) \quad (13)$$

$$\Delta Q^{max}_{PVDG(i)} = min\left(\Delta Q^{IN}_{PVDG(i)}, \Delta Q^{PF}_{PVDG(i)}\right) \quad (14)$$

Figure 6. Structure of ANFIS-RPAC.

3.3. ANFIS-Based PVDG Active Power Curtailment Controller

Although reactive power is important for voltage regulation when intermittent distributed generators are present, its effectiveness is limited by the low *X/R* ratio in power distribution grids and the power factor constraint. Thus, the ratio of voltage magnitude to active power is significantly higher than the ratio of voltage magnitude to reactive power. When the ANFIS-OC algorithm struggles to regulate the voltage magnitude, it will cause the OLTC to experience continuous tap operation.

The suggested ANFIS-based DG active power curtailment controller will compute the optimal active power setpoint in order to reduce the gap between V_{max} and V_{min}, allowing the OLTC to operate in normal conditions. Figure 7 shows the proposed ANFIS-based DG active power curtailment controller (ANFIS-APCC). The controller has two inputs: the maximum voltage magnitude V_{max} of the distribution grid and an array of voltage magnitudes at the DG terminals $V_{PVDG}(i)$. The output $\Delta P_{PVDG}(i)$ is the active power curtailment setpoint provided for a specified PV$DG(i)$. According to their relative contributions to the voltage regulation problem, all PVDGs are subject to different active power curtailment setpoints.

Figure 7. Structure of ANFIS-APCC.

MATLAB/Simulink simulations were conducted to collect the necessary data to train the proposed ANFIS control algorithms. This set of data, which shows the dynamic properties of the active distribution grid, will be divided into three distinct samples. The first sample, which contains 70% of the data, will serve to train the ANFIS controllers. The other 30% of data is equally divided between the other two samples in order to test and validate the models.

Comparing multiple input Membership Functions has found that triangular MFs produce the most desirable outcome. The structure of the fuzzy inference system is defined using the grid partitioning approach. This approach generates input membership functions by uniformly partitioning the input data and producing a single output. This output

represents the OLTC reference voltage computed by the first controller, the reactive power adjustment setpoint in the second controller, and the active power curtailment setpoint in the last. A combination of back-propagation and least squares estimation techniques were used to train both ANFIS control algorithms.

In the proposed method, data is transmitted from the central controller located at the substation to the OLTC controller and to the remote controllers at each PVDG unit. Since this paper focuses on control algorithms, the communication infrastructure to transmit the data is considered ideal and thus not relevant to this study.

3.4. Methodology for Coordinating the ANFIS Algorithm

To prevent tap hunting on the OLTC and to minimize the PVDG active power reduction, the proposed ANFIS controllers must work in coordination with each other. Figure 8 is a flowchart presenting the suggested coordination strategy for managing the two ANFIS controllers.

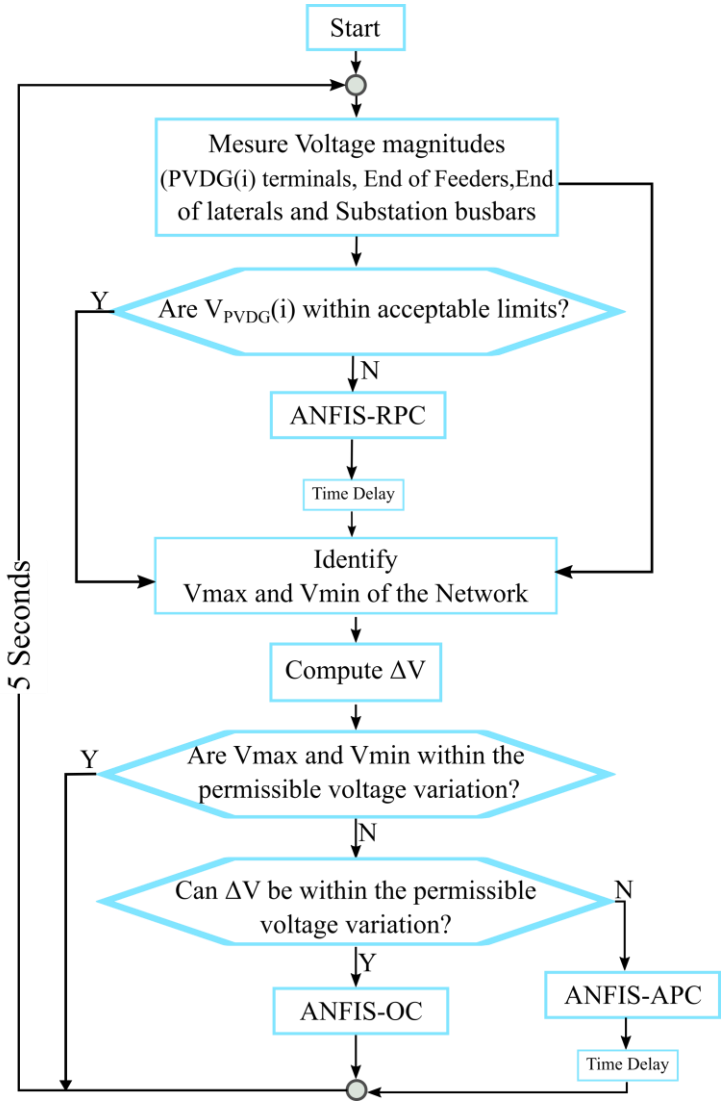

Figure 8. Flowchart of the proposed ANFIS coordination.

The initial step in the proposed process involves identifying and monitoring all critical locations that could potentially experience voltage violations. Next, the voltage at points of interconnection with PVDGs should be examined. When the voltage $V_{PVDG}(i)$ at these points deviates from acceptable bounds, the ANFIS-RPAC calculates the required reactive

power adjustment to regulate and support the voltage. Following this, the maximum voltage (V_{max}) and minimum voltage (V_{min}) across all critical locations are determined. V_{max} is then compared with an upper bound (V_{upper}), and V_{min} is contrasted with a lower bound (V_{lower}). If the range between V_{max} and V_{min} is smaller than the range between V_{upper} and V_{lower}, the ANFIS-OC is activated to ascertain the appropriate reference voltage that would ensure all bus voltages fall within the standard range. However, if this condition is not met, the ANFIS-APCC is brought into action to calculate a new active power curtailment set point. This coordination process is iterated to ensure that voltage magnitudes consistently remain within the standard range. The total update time for the proposed coordination algorithm is set at 5 s. This approach ensures a responsive and dynamic system that adapts to the ongoing changes in the grid.

4. Simulation Results and Discussion

The proposed algorithm is tested using a modified IEEE 33-bus 20 kV PDG, depicted in Figure 9 The substation consists of a 100-MVA power transformer equipped with an OLTC. The substation bus supplies one feeder that has three lateral lines. The network line impedance data is taken from [38]. The load profiles present in the network are a combination of industrial, commercial, and residential types, as illustrated in Figure 10a. Feeder 1 has one PVDG placed at bus 4, whereas lateral line 2 has two PVDGs placed at buses 29 and 33, respectively. The capacity of the PV inverters is set at 14.73 MVA, whereas the peak capacity of the PV panels is 14 MW. The OLTC parameters of all simulation scenarios are detailed in the Appendix A.

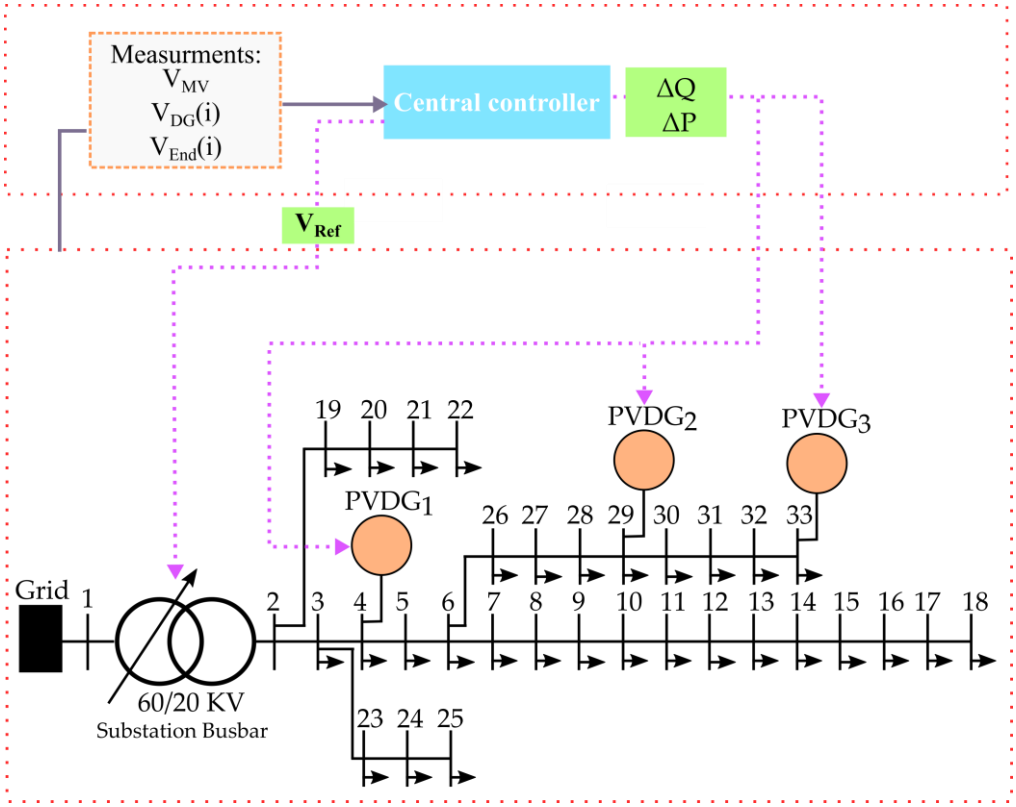

Figure 9. Structure of the modified IEEE 33-bus power distribution grid.

To illustrate the dynamic responsiveness of the proposed methodology, the distribution system is subject to rigorous testing by rapid solar irradiance changes caused by fluctuating cloud conditions, as displayed in Figure 10b.

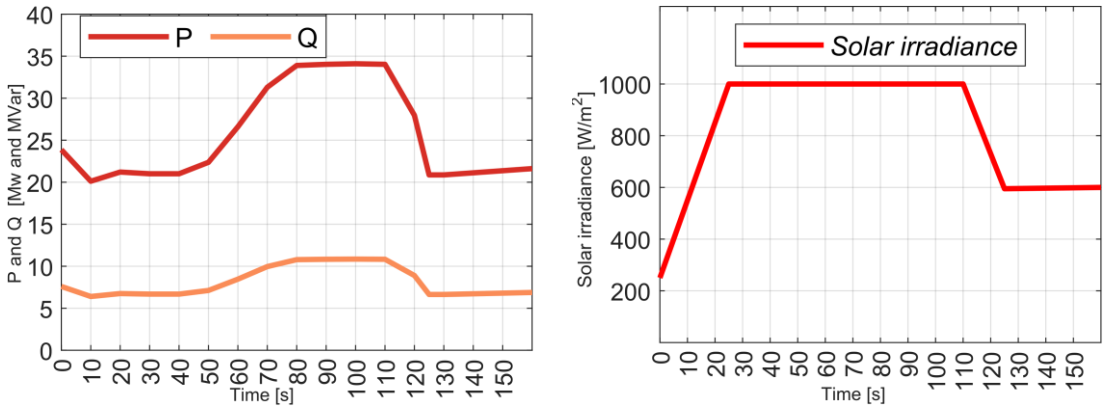

(**a**) (**b**)

Figure 10. Network load profile and solar irradiance. (**a**) Network load profile; (**b**) Solar irradiance.

4.1. Simulation of the Traditional OLTC Voltage Regulation Method

The traditional method will be used to assess the state of the power grid. In this method, the OLTC uses a predefined and constant value to regulate the voltage of the substation bus. Figure 11 displays the obtained results, and Table 1 shows the state of the distribution grid.

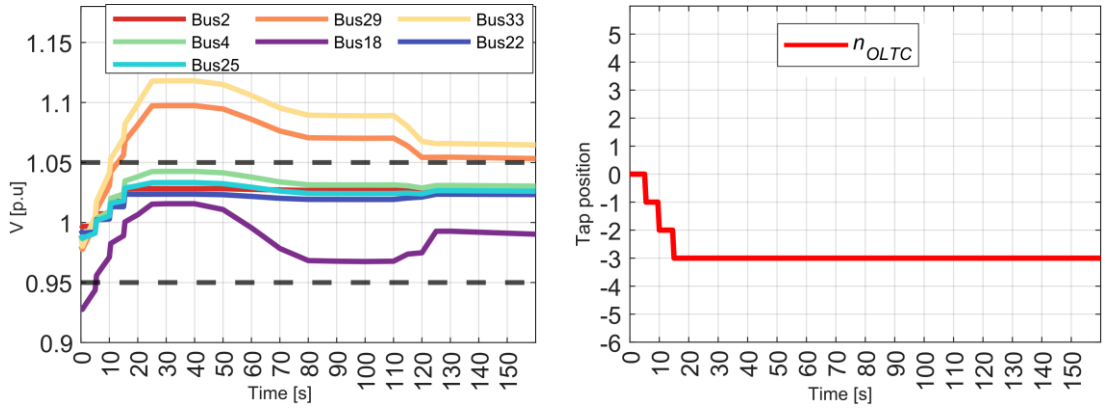

(**a**) (**b**)

Figure 11. Voltage profiles at measured locations and the tap operations of the traditional method. (**a**) Voltage profiles; (**b**) Tap position.

Initially, in the simulation, all the PV inverters operated at a unity power factor. At this particular starting point, the solar irradiance exhibits an intensity of 250 W/m^2, as shown in Figure 10b, considering that the active/reactive powers of the three PVDGs are set to 3.5 MW/0 MVar. This means all voltages at the measured sites are within the allowed range, except the voltage at the last bus of feeder one, which was 0.927 p.u. (see Figure 11a). Since the voltage at the substation bus measured 0.99 p.u. and the reference voltage is set to 1.03 p.u., the OLTC regulated the substation bus voltage magnitude to 1.028 p.u., which falls in the deadband. In Figure 11b, at t = 15 s, after three transformer tap changes (from 0 to −3), all network voltages return to the allowable limit except for the voltages at the PCC of PVDG2 and PVDG3. This is due to a surge in solar irradiance intensity to 700 W/m^2, leading to higher voltage levels at these points.

Table 1. Grid state with the traditional method.

Time (s)	V_{bus2} (p.u.)	V_{bus4} (p.u.)	V_{bus29} (p.u.)	V_{bus33} (p.u.)	V_{bus18} (p.u.)	Tap Position
0	0.99	0.98	0.98	0.98	0.927	0
15	1.028	1.03	1.06	1.08	1	−3
25	1.02	1.04	1.09	1.11	1.01	−3
80	1.02	1.03	1.07	1.08	0.97	−3
125	1.02	1.03	1.05	1.06	0.99	−3

At t = 25 s, when solar irradiance reaches 1000 W/m^2, the active power output of PVDG1, PVDG2, and PVDG3 increases to 14 MW/0 MVAr. This leads to voltage levels at PVDG1a and PVDG2 terminals exceeding the permissible range (an extreme operation, as detailed in Table 1). Concurrently, the voltage magnitude at the substation bus remains equal to 1.028 p.u. As a result, the OLTC is unable to lower the voltage below 1.05 p.u. at these affected locations.

At t = 80 s, with an increase in network load (refer to Figure 10a), the voltage at bus 18 dips to 0.978 p.u. The voltages at PVDG2 and PVDG3 also decline, although they remain above the upper limit. Despite these changes, the substation bus voltage persists within the deadband, indicating the OLTC's inefficacy in regulating the voltage magnitudes at all points of voltage violation.

Towards the simulation end (starting from t = 125 s), a reduction in both solar irradiance (to 600 W/m^2) and load profile was observed, despite the persistently high penetration level. Despite these changes, voltages at PVDG2 and PVDG3 remain above the upper threshold. Meanwhile, the substation bus voltage is equal to 1.02 p.u., implying no change in the OLTC tap position. This suggests that the OLTC still fails to adequately regulate the network voltages.

This dynamic simulation clearly illustrates the limitations of conventional methods that employ fixed references for regulating voltage violations in a distribution grid subject to solar irradiance fluctuations.

4.2. Simulation of ANFIS-OC and Coordination Voltage Regulation Methods

In the subsequent section, we will evaluate the performance of the standalone Adaptive Neuro-Fuzzy Inference System-Optimal Control (ANFIS-OC) and compare it with our proposed method, which involves a coordinated algorithm integrating two additional controllers. These assessments are carried out under identical operating conditions as outlined in the previous section. Figures 12–15 provide a graphical representation of our simulation results, while Tables 2 and 3 give insight into the state of the grid as regulated by both the standalone ANFIS-OC and the proposed coordinated algorithm method, respectively.

In the previous simulation, the voltage magnitude at the substation bus was initially observed to be 0.998 p.u., while the voltage at the end of feeder one dropped to 0.927 p.u., falling below the lower limit (as shown in Figures 12a and 13a). Both methods detected this voltage deficit and computed a new voltage reference of 1.01 p.u., as depicted in Figure 14. Consequently, in both the standalone and coordinated methods, the OLTC executed a single tap operation (changing from 0 to −1), as illustrated in Figures 12b and 13b. This intervention led to an improvement in the voltage level at the termination of feeder one to 0.956 p.u., as reported in Tables 2 and 3.

As the solar irradiance increased between t = 15 s and t = 25 s, a concurrent rise in active power and voltage at the PCC of the PVDG units was noted. The ANFIS-OC managed to restore the voltage at the PCC of PVDG2 following three tap operations, although the voltage at the PCC of PVDG3 remained above the admissible limit. On the contrary, the coordinated method is able to keep all voltages at acceptable levels.

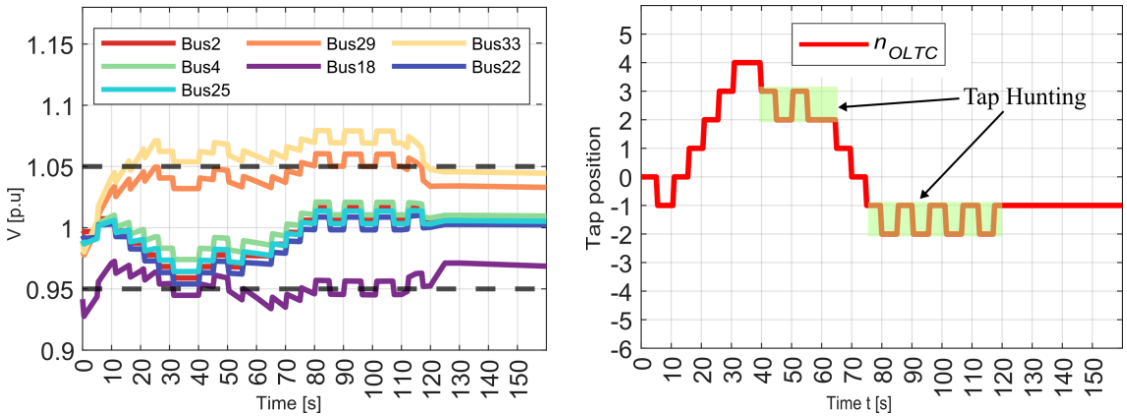

(**a**) (**b**)

Figure 12. Voltage profiles at measured locations and the tap operations of the proposed ANFIS-OC algorithm. (**a**) Voltage profiles; (**b**) Tap position.

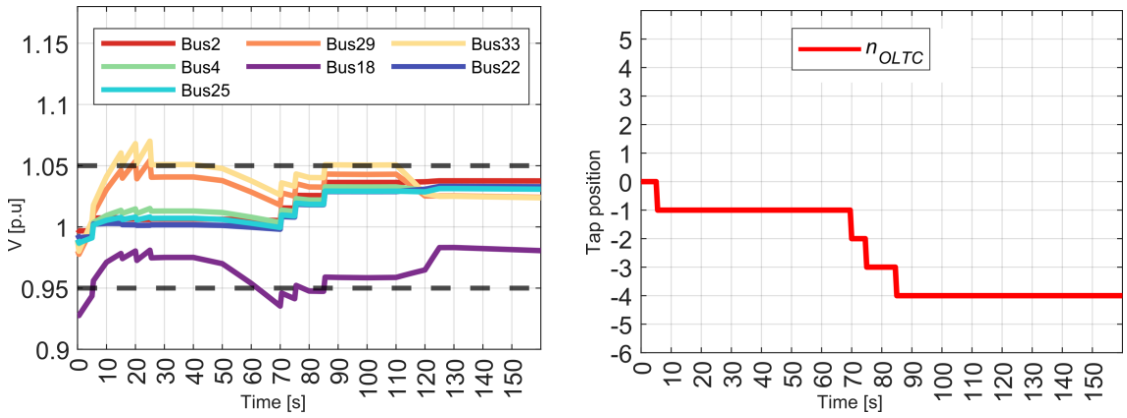

(**a**) (**b**)

Figure 13. Voltage profiles at measured locations and the tap operations of the proposed coordination algorithm. (**a**) Voltage profiles; (**b**) Tap position.

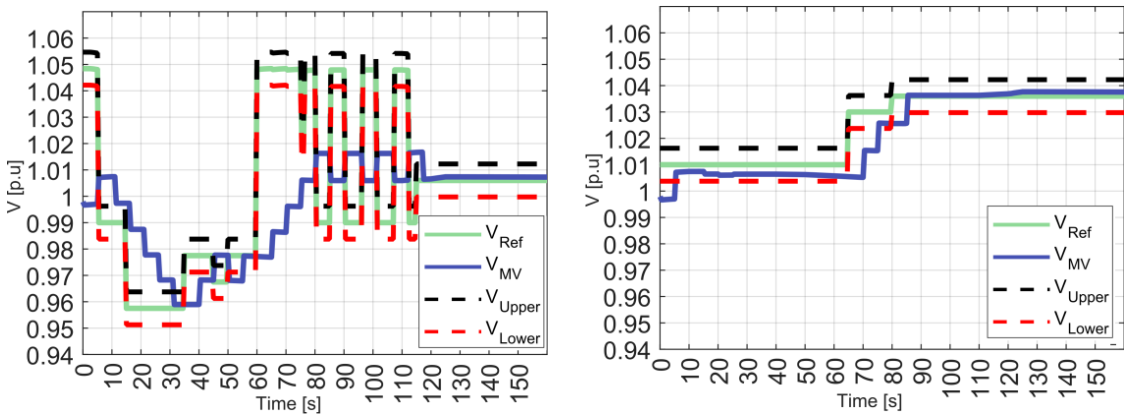

(**a**) (**b**)

Figure 14. The reference voltages proposed by ANFIS-OC and the coordination algorithms. (**a**) The reference voltage calculated by the ANIFS-OC; (**b**) The reference voltage calculated by coordination algorithms.

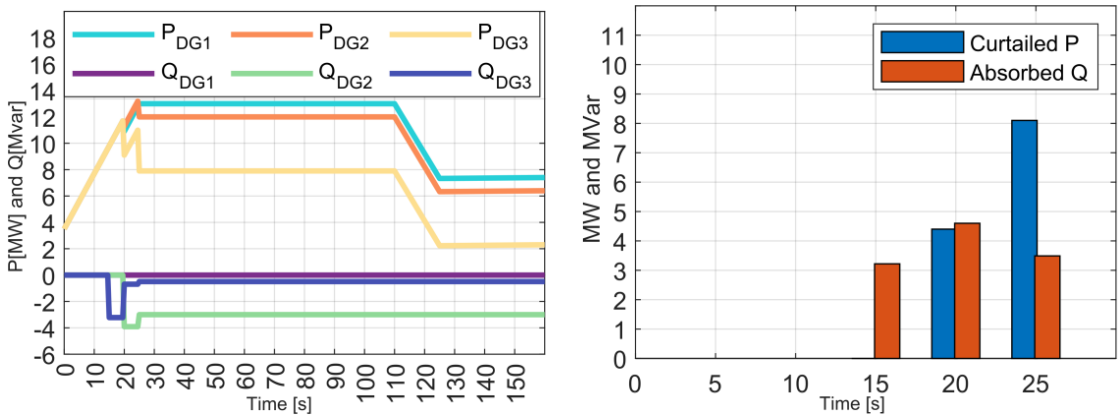

(**a**) (**b**)

Figure 15. The operation curves and the total active power curtailment and reactive power absorption. (**a**) The operation curves of the sources; (**b**) Active power curtailment and reactive power absorption by the PVDG units.

Table 2. Grid state with the proposed ANFIS-OC algorithm.

Time (s)	V_{bus2} (p.u.)	V_{bus4} (p.u.)	V_{bus29} (p.u.)	V_{bus33} (p.u.)	V_{bus18} (p.u.)	Tap Position
0	0.99	0.97	0.97	0.98	0.92	0
5	1	1	1.01	1.01	0.95	−1
15	0.99	1	1.03	1.05	0.96	1
20	0.98	0.99	1.04	1.06	0.96	1
70	0.98	0.99	1.04	1.06	0.93	1
80	1.01	1.02	1.06	1.07	0.95	−2
85	1.01	1.02	1.06	1.07	0.95	−1
125	1	1.01	1.03	1.04	0.97	−1

Table 3. Grid state with the proposed coordination algorithm.

Time (s)	V_{bus2} (p.u.)	V_{bus4} (p.u.)	V_{bus29} (p.u.)	V_{bus33} (p.u.)	V_{bus18} (p.u.)	Tap Position
0	0.99	0.97	0.97	0.98	0.92	0
5	1	1	1.01	1.01	0.95	−1
15	1	1.01	1.03	1.05	0.97	−1
20	1	1.01	1.03	1.05	0.97	−1
25	1	1.01	1.04	1.05	0.94	−1
65	1	1	1.02	1.03	0.94	−1
70	1.01	1.01	1.02	1.03	0.93	−2
75	1.02	1.02	1.03	1.04	0.95	−3
85	1.03	1.03	1.04	1.05	0.95	−4
125	1.03	1.03	1.02	1.02	0.98	−4

Initially, at t = 15 s, PVDG3 absorbed reactive power up to 3.22 MVar (as illustrated in Figure 15a,b), which led to a decrease in voltage at the PCC of PVDG3 to 1.05 p.u. (as demonstrated in Figure 13a). Subsequently, at t = 20 s, all PVDG units participated in

voltage recovery by collectively absorbing reactive power of 4.6 MVar, with ΔQ_{PVDG2} and ΔQ_{PVDG3} being 0.69 MVar and 3.91 MVar, respectively. Additionally, the active power was curtailed by 4.4 MW, split among the PVDG units as follows: ΔP_{PVDG1} reduced by 1 MW, ΔP_{PVDG2} reduced by 0.6 MW, and ΔP_{PVDG1} reduced by 2.8 MW. Finally, at t = 25 s, another round of reactive power absorption and active power reduction took place. This time, an additional 3.49 MVar of reactive power was absorbed, with ΔQ_{PVDG2} and ΔQ_{PVDG3} absorbing 3 MVar and 0.49 MVar, respectively. Active power is further reduced by 8.1 MW, with ΔP_{PVDG2} and ΔP_{PVDG3} experiencing reductions of 2 MW and 6.1 MW, respectively. During periods of high PV use, the coordinated method demonstrated superior performance compared to the standalone ANFIS-OC, indicating the benefit of using coordinated multi-controller approaches in managing complex power grids.

At t = 65 s, the network's rising load profile caused a dip in voltage at bus 18 to 0.944 p.u. However, although the ANFIS-OC succeeded in restoring the voltage on this bus, it was unable to lower the voltages at buses 19 and 33. In contrast, the coordinated method managed to restore all voltages by carrying out tap operations (from -1 to -3) to derive a new V_{ref} value. This was achieved in combination with the reactive power absorption and active power curtailment between t = 15 s and t = 25 s.

From t = 80 s to t = 110 s, when the peak load profile was attained amidst sustained maximum solar irradiance, buses 29 and 33 were subject to overvoltage, while bus 18 experienced undervoltage. This situation led to ANFIS-OC being entrapped in an endless loop, triggering the On-Load Tap-Changer (OLTC) to enter an endless tapping hunt, as illustrated in Figure 15. However, the proposed coordination method succeeded in restoring the voltages with the assistance of the reactive power absorption and active power curtailment that took place between t = 15 s and t = 25 s and through one tap operation (from -3 to -4). Toward the simulation end (starting from t = 125 s), a decline in both solar irradiance (to 600 W/m^2) and the load profile was observed, bringing all voltages within the allowable range.

From these observations, it is evident that the central coordination controller is capable of maintaining voltage levels within the allowable range of a distribution grid. It can prevent continuous OLTC tap operation and minimize active power curtailment under various conditions.

5. Conclusions

In order to maintain voltage stability in a modified IEEE 33-bus distribution grid with a low X/R ratio that experiences voltage violations due to the connection of intermittent PVDGs, an algorithm for managing three ANFIS-based controllers is suggested. The first controller (ANFIS-OC) changes the traditional method by computing the OLTC reference voltage based on the grid's minimum and maximum voltage magnitudes. An auxiliary controller for reactive power control (ANFIS-RPAC) is used to regulate the voltage at the CCP with the power grid in order to prevent the more tap operation of OLTC and to have a small reduction in active power produced by PVDGs. In the case where the difference between these voltage magnitudes exceeds the difference between the upper and lower voltage bounds and the PV inverter reaches its maximum reactive power adjustment, the last proposed controller, ANFIS-APCC, curtails the active power of PVDGs as a means to restore the voltage and to prevent continuous OLTC tap hunting. To examine the effectiveness of the suggested methodology, a MATLAB/SIMULINK simulation of a modified IEEE 33-bus power distribution grid was used.

The integrated coordination control system demonstrated effective management of grid voltages. The first prominent example of this was between t = 15 s and t = 25 s, where all PVDG units played a role in voltage regulation. In addition, between t = 80 s and t = 110 s, an extreme voltage condition was observed, during which the coordination method proved its efficiency in regulating voltages.

These findings, among others, serve as clear evidence of the system's effectiveness. The proposed methodology for coordinating the three ANFIS-based controllers successfully

managed the voltage magnitudes within an active distribution grid. The implications of these findings are significant, suggesting that such a system can maintain stable grid operation even under dynamic conditions.

Author Contributions: Conceptualization, Y.M.; methodology, Y.M.; software, Y.M. and O.B.; validation, H.C., V.P. and R.L.; formal analysis, Y.M.; writing—original draft preparation, Y.M.; writing—review and editing, Y.M., R.L. and V.P.; visualization, V.P.; supervision, R.L. All authors have read and agreed to the published version of the manuscript.

Funding: This research received no external funding.

Data Availability Statement: The data presented in this study are available in the result and discussion section and Appendix A.

Conflicts of Interest: The authors declare no conflict of interest.

Appendix A

Table A1. On-Line Tap Changer parameters.

Voltage Ratings (KV)	**20 KV $\pm$ 8 $\times$ 0.01**
Deadband (p.u.)	0.0125
Voltage step per tap (p.u.)	0.01
Total taps ($2n_{max} + 1$)	17
Tap selection time (s)	5

References

1. Li, C.; Disfani, V.R.; Haghi, H.V.; Kleissl, J. Optimal Voltage Regulation of Unbalanced Distribution Networks with Coordination of OLTC and PV Generation. In Proceedings of the 2019 IEEE Power & Energy Society General Meeting (PESGM), Atlanta, GA, USA, 4–8 August 2019; pp. 1–5.
2. Moldovan, C.; Damian, C.; Georgescu, O. Voltage Level Increase in Low Voltage Networks through Reactive Power Compensation Using Capacitors. *Procedia Eng.* **2017**, *181*, 731–737. [CrossRef]
3. Mahmud, M.A.; Hossain, M.J.; Pota, H.R. Analysis of Voltage Rise Effect on Distribution Network with Distributed Generation. *IFAC Proc. Vol.* **2011**, *44*, 14796–14801. [CrossRef]
4. Choukri, L.; Chekenbah, H.; Lasri, R.; Bouhorma, M.; Maataoui, Y. On-Load Tap-Changer Control by a Fuzzy Logic Controller. In Proceedings of the 2019 4th World Conference on Complex Systems (WCCS), Ouarzazate, Morocco, 22–25 April 2019; pp. 1–6.
5. Wanik, M.Z.C.; Bukshaisha, M.M.; Chaudhry, S.R. PV Generation in Distribution Network and Its Impact on Power Transformer On-Load Tap Changer Operation. In *2017 IEEE Manchester PowerTech*; IEEE: Manchester, UK, 2017; pp. 1–6.
6. Dulău, L.I.; Abrudean, M.; Bică, D. Effects of Distributed Generation on Electric Power Systems. *Procedia Technol.* **2014**, *12*, 681–686. [CrossRef]
7. Sun, W.; Zou, G.; Qiao, S.; Du, X. A Novel Voltage Regulation Scheme for Active Distribution Grid. In Proceedings of the 2020 5th Asia Conference on Power and Electrical Engineering (ACPEE), Chengdu, China, 4–7 June 2020; pp. 493–497.
8. Paudyal, S.; Bhattarai, B.P.; Tonkoski, R.; Dahal, S.; Ceylan, O. Comparative Study of Active Power Curtailment Methods of PVs for Preventing Overvoltage on Distribution Feeders. In Proceedings of the 2018 IEEE Power & Energy Society General Meeting (PESGM), Portland, OR, USA, 5–10 August 2018; pp. 1–5.
9. Iioka, D.; Fujii, T.; Orihara, D.; Tanaka, T.; Harimoto, T.; Shimada, A.; Goto, T.; Kubuki, M. Voltage Reduction Due to Reverse Power Flow in Distribution Feeder with Photovoltaic System. *Int. J. Electr. Power Energy Syst.* **2019**, *113*, 411–418. [CrossRef]
10. Ali, M.S.; Haque, M.M.; Wolfs, P. A Review of Topological Ordering Based Voltage Rise Mitigation Methods for LV Distribution Networks with High Levels of Photovoltaic Penetration. *Renew. Sustain. Energy Rev.* **2019**, *103*, 463–476. [CrossRef]
11. Ren, B.; Zhang, M.; An, S.; Sun, X. Local Control Strategy of PV Inverters for Overvoltage Prevention in Low Voltage Feeder. In Proceedings of the 2016 IEEE 11th Conference on Industrial Electronics and Applications (ICIEA), Hefei, China, 5–7 June 2016; pp. 2071–2075.
12. Newaz, A.; Ospina, J.; Faruque, M.O. Coordinated Voltage Control in Distribution Systems with Distributed Generations. In Proceedings of the 2019 IEEE Power & Energy Society General Meeting (PESGM), Atlanta, GA, USA, 4–9 August 2019; pp. 1–5.
13. Guo, Y.; Wu, Q.; Gao, H.; Chen, X.; Ostergaard, J.; Xin, H. MPC-Based Coordinated Voltage Regulation for Distribution Networks with Distributed Generation and Energy Storage System. *IEEE Trans. Sustain. Energy* **2019**, *10*, 1731–1739. [CrossRef]
14. Mahdavi, S.; Dimitrovski, A. Coordinated Voltage Regulator Control in Systems with High-Level Penetration of Distributed Energy Resources. In Proceedings of the 2019 North American Power Symposium (NAPS), Wichita, KS, USA, 13–15 October 2019; pp. 1–6.

15. Mohiuddin, S.M.; Qi, J. Optimal Distributed Control of AC Microgrids With Coordinated Voltage Regulation and Reactive Power Sharing. *IEEE Trans. Smart Grid* **2022**, *13*, 1789–1800. [CrossRef]
16. Newaz, A.; Ospina, J.; Faruque, O. Controller Hardware-in-the-Loop Validation of Coordinated Voltage Control Scheme for Distribution Systems Containing Inverter-Based Distributed Generation. *IEEE J. Emerg. Sel. Top. Ind. Electron.* **2022**, *3*, 332–341. [CrossRef]
17. Xie, Q.; Shentu, X.; Wu, X.; Ding, Y.; Hua, Y.; Cui, J. Coordinated Voltage Regulation by On-Load Tap Changer Operation and Demand Response Based on Voltage Ranking Search Algorithm. *Energies* **2019**, *12*, 1902. [CrossRef]
18. Joseph, A.; Smedley, K.; Mehraeen, S. Secure High DER Penetration Power Distribution via Autonomously Coordinated Volt/VAR Control. *IEEE Trans. Power Deliv.* **2020**, *35*, 2272–2284. [CrossRef]
19. Hu, R.; Wang, W.; Wu, X.; Chen, Z.; Jing, L.; Ma, W.; Zeng, G. Coordinated Active and Reactive Power Control for Distribution Networks with High Penetrations of Photovoltaic Systems. *Sol. Energy* **2022**, *231*, 809–827. [CrossRef]
20. Mahmud, I.; Masood, N.-A.; Jawad, A. Optimal Deloading of PV Power Plants for Frequency Control: A Techno-Economic Assessment. *Electr. Power Syst. Res.* **2023**, *221*, 109457. [CrossRef]
21. Yazdi, S.S.H.; Rahimi, T.; Haghighian, S.K.; Gharehpetian, G.B.; Bagheri, M. Over-Voltage Regulation of Distribution Networks by Coordinated Operation of PV Inverters and Demand Side Management Program. *Front. Energy Res.* **2022**, *10*, 920654. [CrossRef]
22. Zeraati, M.; Golshan, M.E.H.; Guerrero, J.M. Distributed Control of Battery Energy Storage Systems for Voltage Regulation in Distribution Networks with High PV Penetration. *IEEE Trans. Smart Grid* **2018**, *9*, 3582–3593. [CrossRef]
23. Tonkoski, R.; Lopes, L.A.C.; El-Fouly, T.H.M. Coordinated Active Power Curtailment of Grid Connected PV Inverters for Overvoltage Prevention. *IEEE Trans. Sustain. Energy* **2011**, *2*, 139–147. [CrossRef]
24. Jang, J.-S.R. ANFIS: Adaptive-Network-Based Fuzzy Inference System. *IEEE Trans. Syst. Man Cybern.* **1993**, *23*, 665–685. [CrossRef]
25. Spatti, D.H.; da Silva, I.N.; Usida, W.F.; Flauzino, R.A. Real-Time Voltage Regulation in Power Distribution System Using Fuzzy Control. *IEEE Trans. Power Deliv.* **2010**, *25*, 1112–1123. [CrossRef]
26. Spatti, D.H.; da Silva, I.N.; Usida, W.F.; Flauzino, R.A. Fuzzy Control System for Voltage Regulation in Power Transformers. *IEEE Lat. Am. Trans.* **2010**, *8*, 51–57. [CrossRef]
27. Kakigano, H.; Miura, Y.; Ise, T. Distribution Voltage Control for DC Microgrids Using Fuzzy Control and Gain-Scheduling Technique. *IEEE Trans. Power Electron.* **2013**, *28*, 2246–2258. [CrossRef]
28. Azzouz, M.A.; Farag, H.E.; El-Saadany, E.F. Real-Time Fuzzy Voltage Regulation for Distribution Networks Incorporating High Penetration of Renewable Sources. *IEEE Syst. J.* **2017**, *11*, 1702–1711. [CrossRef]
29. Kim, B.-G.; Rho, D.-S. Optimal Voltage Regulation Method for Distribution Systems with Distributed Generation Systems Using the Artificial Neural Networks. *J. Electr. Eng. Technol.* **2013**, *8*, 712–718. [CrossRef]
30. Mahmud, N.; Zahedi, A.; Mahmud, A. A Cooperative Operation of Novel PV Inverter Control Scheme and Storage Energy Management System Based on ANFIS for Voltage Regulation of Grid-Tied PV System. *IEEE Trans. Ind. Inform.* **2017**, *13*, 2657–2668. [CrossRef]
31. Ratra, S.; Tiwari, R.; Niazi, K.; Bansal, R. Optimal Coordinated Control of OLTCs Using Taguchi Method to Enhance Voltage Stability of Power Systems. *Energy Procedia* **2019**, *158*, 3957–3963. [CrossRef]
32. Gholami, K.; Islam, R.; Rahman, M.; Azizivahed, A.; Fekih, A. State-of-the-Art Technologies for Volt-Var Control to Support the Penetration of Renewable Energy into the Smart Distribution Grids. *Energy Rep.* **2022**, *8*, 8630–8651. [CrossRef]
33. Kasztenny, B.; Rosolowski, E.; Izykowski, J.; Saha, M.; Hillstrom, B. Fuzzy Logic Controller for On-Load Transformer Tap Changer. *IEEE Trans. Power Deliv.* **1998**, *13*, 164–170. [CrossRef]
34. Awad, A.S.A.; Turcotte, D.; EL-Fouly, T.H.M.; Prieur, A. Impact of Distributed Generation on the Operation of Load Tap Changers in Canadian Suburban Benchmark Distribution Network. In Proceedings of the 2017 IEEE 30th Canadian Conference on Electrical and Computer Engineering (CCECE), Windsor, ON, Canada, 12–17 April 2017; pp. 1–5.
35. Razavi, S.-E.; Rahimi, E.; Javadi, M.S.; Nezhad, A.E.; Lotfi, M.; Shafie-khah, M.; Catalão, J.P.S. Impact of Distributed Generation on Protection and Voltage Regulation of Distribution Systems: A Review. *Renew. Sustain. Energy Rev.* **2019**, *105*, 157–167. [CrossRef]
36. Murray, W.; Adonis, M.; Raji, A. Voltage Control in Future Electrical Distribution Networks. *Renew. Sustain. Energy Rev.* **2021**, *146*, 111100. [CrossRef]
37. Azzouz, M.A.; Farag, H.E.; El-Saadany, E.F. Fuzzy-Based Control of on-Load Tap Changers under High Penetration of Distributed Generators. In Proceedings of the 2013 3rd International Conference on Electric Power and Energy Conversion Systems, Istanbul, Turkey, 2–4 October 2013; pp. 1–6.
38. Dolatabadi, S.H.; Ghorbanian, M.; Siano, P.; Hatziargyriou, N.D. An Enhanced IEEE 33 Bus Benchmark Test System for Distribution System Studies. *IEEE Trans. Power Syst.* **2021**, *36*, 2565–2572. [CrossRef]